



Seasonal variability of sediment controls of nitrogen cycling in an agricultural stream

Sophie A. Comer-Warner · Daren C. Goody · Sami Ullah ·
Luke Glover · Nicholas Kettridge · Sarah K. Wexler · Jan Kaiser ·
Stefan Krause

Received: 18 March 2019 / Accepted: 1 February 2020
© The Author(s) 2020

Abstract Agricultural streams receive large inputs of nutrients, such as nitrate (NO_3^-) and ammonium (NH_4^+), which impact water quality and stream health. Streambed sediments are hotspots of biogeochemical reactivity, characterised by high rates of nutrient attenuation and denitrification. High concentrations of nitrous oxide (N_2O) previously observed in stream sediments point to incomplete denitrification, with sediments acting as a potentially significant source of global N_2O . We investigated the effect of sediment type and seasonal variation on denitrification and N_2O production in the streambed of an agricultural UK stream. Denitrification was strongly controlled by sediment type, with sand-dominated sediments exhibiting potential rates of denitrification

almost 10 times higher than those observed in gravel-dominated sediments ($0.026 \pm 0.004 \text{ N}_2\text{O-N } \mu\text{g g}^{-1} \text{ h}^{-1}$ for sand-dominated and $0.003 \pm 0.003 \text{ N}_2\text{O-N } \mu\text{g g}^{-1} \text{ h}^{-1}$ for gravel-dominated). In-situ measurements supported this finding, with higher concentrations of NO_3^- , nitrite (NO_2^-) and N_2O observed in the porewaters of gravel-dominated sediments. Denitrification varied substantially between seasons, with denitrification increasing from winter to autumn. Our results indicate highest NO_3^- reduction occurred in sand-dominated sediments whilst highest N_2O concentrations occurred in gravel-dominated sediments. This suggests that finer-grained streambeds could play an important role in removing excess nitrogen from agricultural catchments without producing excess N_2O .

Responsible Editor: Edward Brzostek.

Electronic supplementary material The online version of this article (<https://doi.org/10.1007/s10533-020-00644-z>) contains supplementary material, which is available to authorized users.

S. A. Comer-Warner · S. Ullah · N. Kettridge ·
S. Krause
School of Geography, Earth and Environmental Sciences,
University of Birmingham, Edgbaston,
Birmingham B15 2TT, UK
e-mail: s.comer-warner@bham.ac.uk

D. C. Goody
British Geological Survey (BGS), Maclean Building,
Wallingford, Oxfordshire OX10 8BB, UK

S. Ullah · L. Glover
School of Geography, Geology and the Environment,
University of Keele, Keele, Newcastle ST5 5BG, UK

S. K. Wexler · J. Kaiser
Centre for Ocean and Atmospheric Sciences, School of
Environmental Sciences, University of East Anglia,
Norwich Research Park, Norwich NR4 7TJ, UK

Introduction

Large inputs of nutrients, such as nitrate (NO_3^-) and ammonium (NH_4^+), transported to freshwater ecosystems either directly or through subsurface flows, severely impact ecosystem health and functioning in many agricultural lowland streams (Krause et al. 2009; Pinay et al. 2015, 2018; Smith et al. 1999). This is due to high nitrogen (N) concentrations, which often lead to eutrophication, causing a reduction in oxygen content, water quality, and stream habitats (Brunke and Gonser 1997; Glibert et al. 2005; Kemp et al. 2005; Krause et al. 2009; McMahon and Böhlke 1996; Seitzinger et al. 2002; Sophocleous 2002). Nutrient attenuation within streams may prevent degradation of aquatic ecosystems, however, the processes involved, predominantly nitrification and incomplete denitrification, may also produce the greenhouse gas (GHG) nitrous oxide (N_2O) (Duff et al. 2008; Lansdown et al. 2012; Lansdown et al. 2015; Quick et al. 2016, 2019).

Current estimates of N_2O emissions from rivers predict ranges from 0.1 to 0.68 Tg $\text{N}_2\text{O-N}$ y^{-1} (Anderson et al. 2010; Beaulieu et al. 2011), with the highest estimate equal to approximately 10% of global anthropogenic emissions (Beaulieu et al. 2011). The relative N_2O contributions from streams and rivers in relation to their share of the Earth's surface, $\sim 0.15\%$ (Allen and Pavelsky 2018), indicates that streams and rivers are disproportionately important in global N_2O emissions. It is essential, therefore, to understand drivers and controls of N_2O emissions from aquatic-atmospheric interfaces, especially as it is a GHG approximately 298 times more potent than CO_2 on a mole per mole basis (Forster et al. 2007), with a large ozone-depleting potential compared to other ozone-depleting compounds of anthropogenic origin (Ravishankara et al. 2009).

Within streams and rivers, streambed sediments have been identified as hotspots of biogeochemical reactivity (Krause et al. 2013; Lautz and Fanelli 2008; McClain et al. 2003; Trimmer et al. 2012; Shelley et al. 2017), due to observations of increased residence time and substrate (e.g. carbon (C), N) availability within these environments (Boulton et al. 1998; Grimm and Fisher 1984; Mulholland et al. 2000; Pinay et al. 2009; Zarnetske et al. 2011). Streambed sediments, therefore, have the potential to cause significant nutrient attenuation, leading to reductions in NO_3^- concentrations and subsequent improvements in surface water

quality, ecosystem services and ecosystem health (Duff and Triska 2000; Rivett et al. 2008a, b; Wang et al. 2012), however, this may be accompanied by associated N_2O emissions. The controls and drivers of streambed nutrient attenuation and N_2O production are insufficiently understood. Given the potential of streambeds to be a significant source of global N_2O (Beaulieu et al. 2011; Mosier et al. 1998; Mulholland et al. 2008), it is critical to understand the factors controlling N_2O production in streambed sediments (Quick et al. 2016).

Denitrification is a key process of NO_3^- removal in stream sediments. Denitrification rates are usually elevated in the streambed relative to the surface water (Quick et al. 2016). Streambed denitrification is controlled by substrate availability, organic C quality, redox conditions, temperature, enzyme activity and pH (Bakken et al. 2012; Bonin et al. 2002; Codispoti 2010; Findlay 1995; Kaplan and Newbold 2000; Senayram et al. 2012; Silvennoinen et al. 2008a, b; Silvennoinen et al. 2008a, b; Quick et al. 2019). These are further dependent on sediment type, with finer sediments typically characterised by longer residence times, higher presence of C and N and lower dissolved oxygen concentrations, all of which have positive correlations to denitrification rates and N_2O production (Findlay et al. 2011; García-Ruiz et al. 1998; Zarnetske et al. 2015). Sediment type may also affect microbial assemblages and functional capacities (Crawford et al. 2017). Recent work has shown that water residence times in sediments are a key control on denitrification, with short residence times unable to support complete NO_3^- reduction, and long residence times resulting in complete denitrification and associated water quality improvements (Gomez-Velez et al. 2015; Quick et al. 2016; Zarnetske et al. 2011, 2015). In addition to in-stream heterogeneity affecting denitrification and N_2O production there may be large variations in the abundance of sites able to support denitrification, due to factors including variations in available substrate and redox conditions between streams, especially in catchments with differing land-uses (Findlay et al. 2011; García-Ruiz et al. 1998).

Further investigation, therefore, is required to explain the processes and the environmental drivers controlling N_2O production in sediments. Recent work addressing these research questions determined that intermediate residence times lead to incomplete

denitrification, resulting in a reduction in NO_3^- concentration and improvement in water quality, while producing N_2O (Burgin et al. 2013; Quick et al. 2016). For example, an optimal residence time of 9 h for N_2O production was determined in flume experiments containing sand dunes (Quick et al. 2016).

Here we investigate denitrification in a small, agricultural stream, where incomplete denitrification and subsequent N_2O emissions may be disproportionately important due to increased nutrient uptake and processing rates in small streams (Alexander et al. 2000). Incomplete denitrification is particularly important to understand in streams and rivers as this is suggested to be the dominant global pathway of N_2O production (Quick et al. 2019). We hypothesise that N cycling will vary between sediment type (sand-dominated versus gravel-dominated) and season due to differences in available substrate, residence times and temperature. We address these hypotheses through the determination of potential rates of denitrification, in-situ porewater and surface water concentrations and the isotopic composition of $\text{NO}_3^- + \text{NO}_2^-$ ($\delta^{15}\text{N}_{\text{NO}_3^- + \text{NO}_2^-}$ and $\delta^{18}\text{O}_{\text{NO}_3^- + \text{NO}_2^-}$). The combination of concentration and isotopic data provides invaluable information on sources and processes although it should be noted that process rather than source information is more reliable from N isotopes in water (Kendall 1998; Venkiteswaran et al. 2019). These techniques, therefore, were used in conjunction here to provide evidence of whether denitrification is occurring. As sediment type varies greatly within streams, constraining differences in denitrification and N_2O production between varying sediment types is key to understanding stream-wide N cycling. Acknowledging that temporal variability in nutrient loading and temperatures can have substantial impact on biogeochemical processing rates, we furthermore analyse seasonal variability in denitrification and N_2O concentrations to identify potential hot moments in streambed NO_3^- turnover.

Materials and methods

Study site

Experiments were conducted in the Wood Brook (Birmingham Institute of Forest Research,

Staffordshire, UK), which is situated within a mixed-use, agricultural catchment. The predominant catchment use changed during the experimental period and was dominated by cultivated fields (predominantly wheat) in 2016 and grass in 2017, with the rest of the catchment area comprised of young and mature deciduous woodland (Fig. 1a). Fertiliser was applied three times during spring in 2016 at rates of 45 to 80 kg N ha^{-1} and multiple times throughout most of the year in 2017 (January to September) at rates of 10 to 181 kg N ha^{-1} . The catchment geology is Permo-Triassic sandstone overlain by up to 10 m of glacial till deposits, which in turn are overlain by 0.15 to 0.6 m of sandy clay sediment (Blaen et al. 2017).

The experiments of this study were conducted within a 700 m section of the Wood Brook, downstream of an agricultural catchment dominated by cultivated fields and grass ley systems, where the stream flows just within a patch of mature deciduous woodland (Fig. 1a). This resulted in the upstream end of the study area directly bordering the cultivated fields on one side, with the stream being separated from the fields by a narrow strip of woodland further downstream. Within the study area, three smaller sites were identified (Fig. 1a and b), with sand-dominated sediments in sites 1 and 2, and gravel-dominated sediments in site 3. Further site characteristics can be found in Tables 1 and 2, with detailed physical parameters in Table S1. The DO, temperature and dissolved organic carbon (DOC) data were measured in porewater samples taken at the same location, depth and time as samples for N_2O and nutrient analysis. The water depths represent the average depth at each site, however, the water level at some of the gravel sediments in site 3 and the sand sediment at piezometer 4 in site 1 was just below the sediment in summer and autumn.

In-situ measurements

Porewater and surface water samples were collected to investigate in-situ N cycling, and determined concentrations of NH_4^+ , NO_3^- , NO_2^- and N_2O and isotopic values of $\delta^{15}\text{N}_{\text{NO}_3^- + \text{NO}_2^-}$ and $\delta^{18}\text{O}_{\text{NO}_3^- + \text{NO}_2^-}$. Porewater samples were collected manually in July 2016, October 2016, January 2017 and March 2017 from 10 and 20 cm depths below the sediment surface, from multilevel piezometers installed into the streambed at

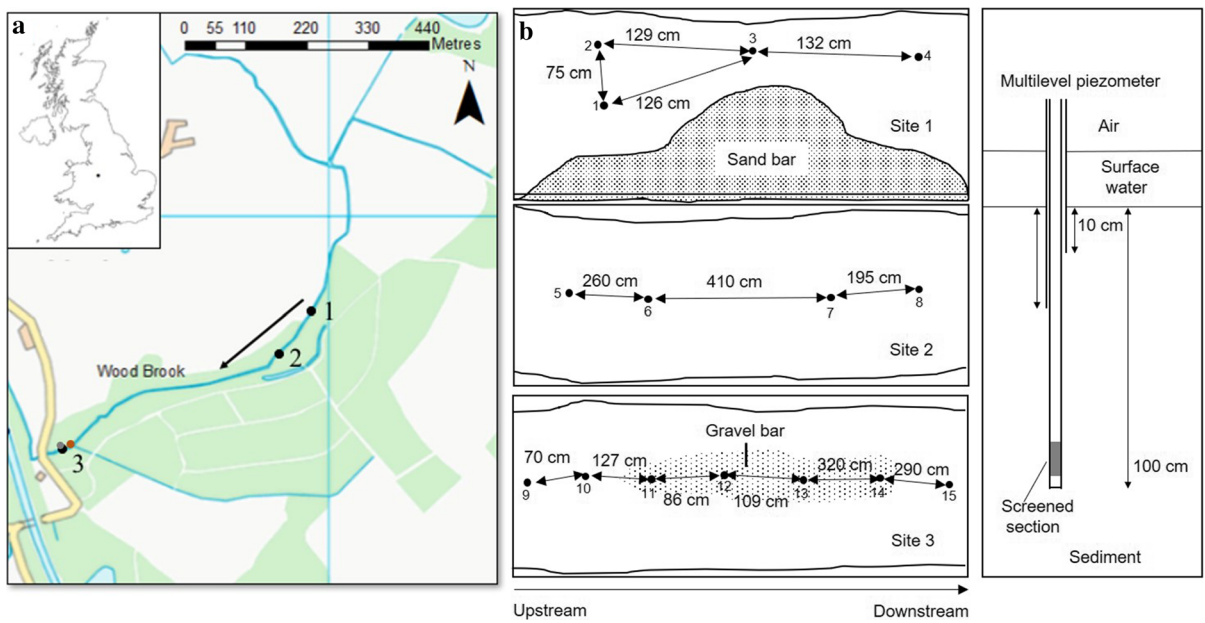


Fig. 1 **a** The location of the Wood Brook within the UK, and the direction of stream flow (black arrow), woodland (green area) and fields (white area) of the Wood Brook and its catchment. The three study sites are represented by the black dots, and the grey and orange circles indicate the site of sampling of sediment representative of gravel-dominated sediments and sand-dominated sediments, respectively. **b** A

diagram of the three experimental sites including shaded areas representing a sand bar at one side of the stream in site 1 and a gravel bar close to the center of the stream in site 3, the positions of the piezometers within the three experimental sites are also shown, and **c** a diagram of the multilevel piezometer set-up with depths of 10 and 20 cm used to sample porewater

Table 1 Average key characteristics from each site

Site	DO (%Sat.)	Temperature (°C)	DOC (mg l ⁻¹)	q _{3D} (d ⁻¹)	OM Content (%)	d (0.9) (μm)
1	31.5	10.8	16.1	42.4	2.9	525.0
2	20.9	11.0	13.2	35.4	1.4	627.1
3	25.9	10.5	13.2	80.5	0.9	812.2

Presented are dissolved oxygen (DO; %), temperature (°C), dissolved organic carbon (DOC; mg l⁻¹), three-dimensional flux of porewater through the streambed (q_{3D}; d⁻¹), sediment organic matter content (OM; % LOI) and grain size of sediment sieved at 2 mm (diameter which encompasses 90% of particles; d; μm). Data for DOC q_{3D} and OM content are taken from Comer-Warner et al. (2019)

three locations (Fig. 1b and c) (Krause et al. 2013; Rivett et al. 2008a, b). A surface water sample was taken at each site at the same time as porewater sampling. The pH and electrical conductivity (Hanna HI98129), and dissolved oxygen concentration and temperature (YSI ProODO or EcoSense ODO200), of the samples were measured *in-situ* (Table S1). Water samples were then filtered (0.45 then 0.22 μm Thames Resteck nylon) into sterile centrifuge tubes and frozen until analysis.

A headspace equilibrium method (McAuliffe 1971) was used in the field prior to filtering of samples to analyse porewater and surface water gas concentrations. 7 ml of water sample was collected in a syringe and 14 ml of ultrapure helium was drawn into the syringe and shaken vigorously for two minutes. The headspace was then collected in a pre-evacuated exetainer (12 ml) and stored at room temperature, in the dark, until analysis.

Nutrient concentrations in the surface water and porewater samples were analysed on a continuous flow

Table 2 Stream discharge ($l\ s^{-1}$) and average water depths (cm) at each site for each season

Season	Site	Discharge ($l\ s^{-1}$)	Average water depth (cm)
Spring	1	39.15	11
	2	38.61	9
	3	40.96	11
Summer	1	14.11	5
	2	14.40	4
	3	15.90	10
Autumn	1	7.85	4
	2	8.19	7
	3	15.06	11
Winter	1	68.09	19
	2	68.95	16
	3	72.06	14

analyser (Skalar San++), and standards of 0.58, 1.00 and 1.00 mg N l^{-1} were analysed for NH_4^+ , NO_3^- and NO_2^- , respectively, to determine machine performance. These standards resulted in an accuracy and precision of 0.03 and ± 0.05 mg N l^{-1} for NH_4^+ , 0.06 and ± 0.05 mg N l^{-1} for NO_3^- , and 0.02 and ± 0.005 mg N l^{-1} NO_2^- , respectively. The limit of detection (LOD) was 0.05, 0.02 and 0.02 mg N l^{-1} , for NH_4^+ , NO_3^- and NO_2^- , respectively.

N_2O concentrations of the gas samples from the incubation and field experiments were measured using a gas chromatograph (GC) (Agilent 7890A) fitted with a micro electron capture detector (μECD). Laboratory and field samples (collected in July) were analysed using a 1 ml sample loop in splitless mode, with an oven temperature of 60 °C, and a μECD temperature of 350 °C. A make-up gas of argon and methane was used with a flow rate of 2 ml min^{-1} , and a run time of 9 min was used, with N_2O eluted at 7 min. The LOD was 0.08 ppm, and a 6.2 ppm standard resulted in an accuracy of 0.1 ppm and a precision of ± 0.2 ppm. All other field samples were analysed on a GC- μECD in splitless mode with a 250 μl sample loop, an oven temperature of 30 °C and a μECD temperature of 300 °C. A make-up gas of N_2 with a flow rate of 30 ml s^{-1} was used, with a run time of 5 min resulting in N_2O eluting at 3 min. The LOD was 5.6×10^{-3} ppm, and a standard of 9.71 ppm resulted in an accuracy of 0.10 ppm and a precision of ± 1.75 ppm. Henry's constant was used to determine the

porewater concentration for all field samples (Hudson 2004; Wilhelm et al. 1977).

Analysis of porewater NO_3^- isotopic composition ($\delta^{15}\text{N}_{\text{NO}_3^-+\text{NO}_2^-}$ and $\delta^{18}\text{O}_{\text{NO}_3^-+\text{NO}_2^-}$) was performed at the Science Analytical Facilities of the University of East Anglia using the denitrifier method (Casciotti et al. 2002; Kaiser et al. 2007; Sigman et al. 2001). Isotope analysis was performed by adjusting aqueous sample volume to contain 2 μM NO_3^- (plus NO_2^- if present), which was converted to N_2O using denitrifying bacteria. The international reference materials for isotopes in NO_3^- ; IAEA NO_3^- , USGS 34 and USGS 35, and an in-house reference containing NO_3^- (river water), were prepared and analysed alongside samples. The isotopic composition of the N_2O was measured on a gas chromatograph isotope ratio mass spectrometer (GEO 20:20), and the $\delta^{15}\text{N}_{\text{NO}_3^-}$ and $\delta^{18}\text{O}_{\text{NO}_3^-}$ of NO_3^- was calculated using calibration to the reference materials USGS 34 and USGS 35. The long-term measurement precision for the in-house reference was ± 0.3 and $\pm 0.4\text{‰}$ for $\delta^{15}\text{N}_{\text{NO}_3^-}$ and $\delta^{18}\text{O}_{\text{NO}_3^-}$ respectively. Accepted values of the international reference materials can be found in Table S2. IAEA- NO_3^- was used as scale anchor with $\delta^{15}\text{N}_{\text{NO}_3^-} = 4.70\text{‰}$ and $\delta^{18}\text{O}_{\text{NO}_3^-} = 25.61\text{‰}$ (Böhlke et al. 2003; Kaiser et al. 2007). The resulting $\delta^{15}\text{N}_{\text{NO}_3^-}$ values for USGS34 and USGS35 were -1.80 and 2.75 ‰, respectively, with $\delta^{18}\text{O}_{\text{NO}_3^-}$ values of -28.20 and 57.27 ‰, respectively. The measurement precision was 0.14, 0.11 and 0.19 ‰ for $\delta^{15}\text{N}_{\text{NO}_3^-}$ of IAEA- NO_3^- , USGS 34 and USGS 35, respectively, and 0.19, 0.37 and 0.59 ‰, respectively, for $\delta^{18}\text{O}_{\text{NO}_3^-}$.

Although incomplete denitrification and nitrification are often the predominant sources of N_2O in soils and hyporheic sediments (Bollmann and Conrad 1998; Davidson 1991; Heppell et al. 2013; Lansdown et al. 2012, 2015a; Quick et al. 2016; Well et al. 2005), other N cycling processes may play important roles (Kelso et al. 1997; Lansdown et al. 2016; Stevens and Laughlin 1998). As only denitrification was considered here the data collected may represent an oversimplification of the system.

Laboratory incubation experiments

Stream sediments were incubated to determine potential rates of denitrification. Sediments were collected during June 2015 from two locations within the streambed (Fig. 1a), representative of the sand-dominated and gravel-dominated sediments found in the experimental sites. The gravel-dominated sediments were collected at site 3, and the sand-dominated sediments were collected 15 m upstream in a section of the stream with woody debris. Sediment samples were collected between 0 and 10 cm depth using an AMS slide hammer (5 cm dia.) and a trowel. Five pseudo-replicates of each sample were collected at each site. Sediment samples were homogenised and sieved (2 mm) within 36 h of collection and stored cold.

Potential rates of denitrification were determined as follows on five replicates from each site. 10 g of field-moist sediment was placed into 100 ml glass serum bottles. The bottles were wrapped in aluminium foil, to simulate dark conditions within the streambed, and then covered in parafilm and stored cold for less than 24 h. The bottles were removed from the refrigerator prior to the incubation experiments to allow the samples to reach room temperature. 20 ml of the relevant stock solution (ultrapure water for the control incubations, 30 mg l⁻¹ NO₃⁻ solution for the NO₃⁻-spiked incubations, 40 mg l⁻¹ glucose solution (concentration as C equivalents) for the C-spiked incubations or a 30 mg l⁻¹ NO₃⁻, 40 mg l⁻¹ glucose-C solution for the mixed substrate incubations) was added to each bottle. The spiking with NO₃⁻ and glucose was used to evaluate whether denitrification was NO₃⁻ and/or C limited under induced anoxic conditions. Following addition of the substrates, the bottles were capped with gas tight rubber septa and then flushed with oxygen-free argon for 30 min to induce anoxic conditions. Following this, 10% of the headspace was replaced with pure acetylene gas to prevent the conversion of N₂O to N₂ (Sgouridis and Ullah 2014). Incubations were performed at 22 °C on a reciprocating shaker at 400 rpm, and 7 ml gas samples were taken from the headspace at zero, three and six hours and injected into 5.6 ml pre-evacuated exetainers. The headspace volume and pressure were maintained throughout the experiment by replacing the removed gas with a 10:1 argon:acetylene mixture after each sampling time.

Analysis of statistical inference

In-situ measurements

The effect of sediment type and season on N cycling was inferred using a linear mixed-effects model fitted using the residual maximum likelihood in the *nlme* package in R (Pinheiro et al. 2017). The data for piezometer 1 at 10 cm was omitted from the statistical analysis as the oxygen data indicated that this sample was surface water, and the inclusion of this data point prevented model residuals from meeting the necessary model assumptions. The data were nested by site and season to account for the sampling repetition in time and the repetition of sampling at each site. Where the model residuals did not fit the Gaussian assumption data were shifted so that any values less than or equal to zero were positive and transformed (\log_{10} , reciprocal or square root) depending on which transformation resulted in the best residual fit. The model was fitted both with (Eq. 1) and without (Eq. 2) the interaction between sediment type and season.

$$y_{ijk} = \mu + \alpha_i + \beta_j + (\alpha\beta)_{ij} + \gamma_i + \gamma_k + \varepsilon_{ijk}, \quad (1)$$

where y_{ijk} is the observation for site i , season j and sample k ; μ is the mean of y ; α_i is the fixed effect for site i ; β_j is the fixed effect for season j ; $(\alpha\beta)_{ij}$ is the interaction fixed effect for site i and season j ; $\gamma_i \sim N(0, \sigma_{\gamma}^2)$ is the random event for site i ; $\gamma_k \sim N(0, \sigma_{\gamma}^2)$ is the random event for the sample and $\varepsilon_{ijk} \sim N(0, \sigma^2)$ is the residual.

$$y_{ijk} = \mu + \alpha_i + \beta_j + \gamma_i + \gamma_k + \varepsilon_{ijk}, \quad (2)$$

where y_{ijk} is the observation for site i , season j and sample k ; μ is the mean of y ; α_i is the fixed effect for site i ; β_j is the fixed effect for season j ; $\gamma_i \sim N(0, \sigma_{\gamma}^2)$ is the random event for site i ; $\gamma_k \sim N(0, \sigma_{\gamma}^2)$ is the random event for the sample and $\varepsilon_{ijk} \sim N(0, \sigma^2)$ is the residual. The Akaike Information Criterion (AIC) was used to compare the models and the model with the lowest AIC was used.

Laboratory incubation experiments

The responses between the sand-dominated and gravel-dominated sediments for each incubation experiment were tested for significant differences using a Welch's Two Sample t-test or the non-parametric equivalent (Wilcoxon Rank Sum Test) where the assumptions of normality and equal variance were violated.

Results

In-situ N cycling

NH_4^+

Porewater NH_4^+ concentrations were consistently highest in sites 1 and 2 during all seasons (Fig. 2a), leading to statistically significant differences between

sites (p value < 0.001, Table S4). NH_4^+ concentrations were highest in autumn, especially in site 2, and were lowest in winter and spring, leading to statistically significant differences between autumn and spring (p value = 0.043, Table S4). NH_4^+ concentrations were higher in the surface water than in the porewaters in sites 1 and 2, but were similar to porewater concentrations in site 3 (Fig. S1).

NO_3^-

Porewater NO_3^- concentrations were consistently highest in sites 1 and 3, and lowest in site 2 throughout all seasons (Fig. 2b), resulting in statistically significant differences between sites (p value < 0.030, Table S4). Variation in NO_3^- concentrations between seasons was low but significant between autumn and winter (p value = 0.005, Table S4). NO_3^- concentrations were lower in the surface water than in the porewaters at all sites (Fig. 3).

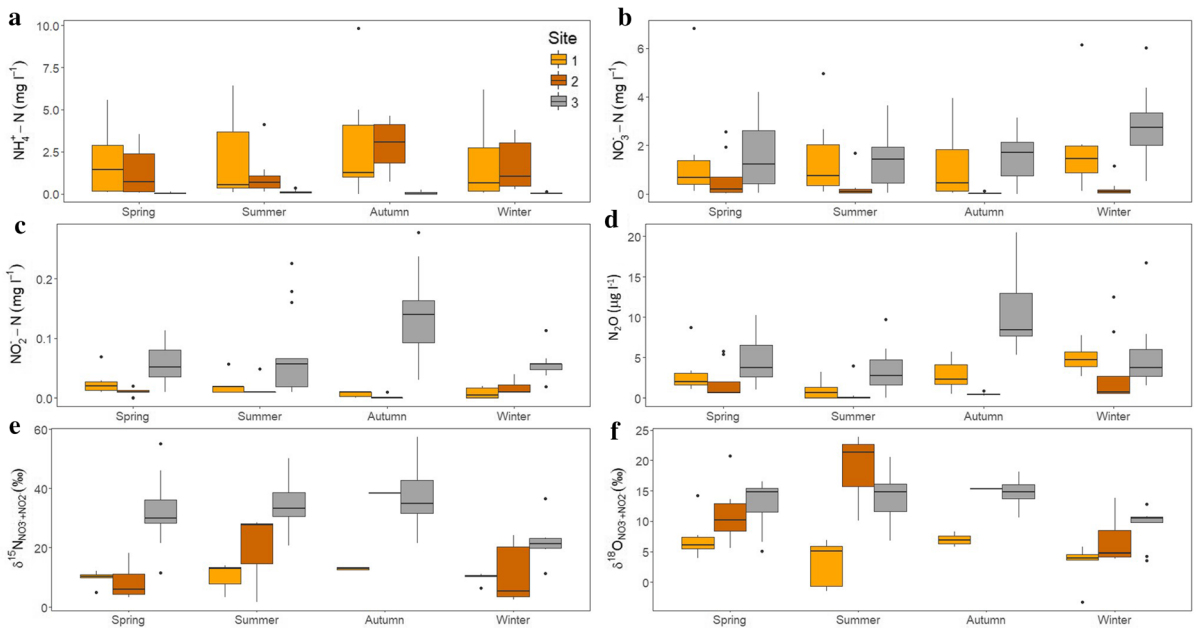


Fig. 2 Boxplots between sites and across seasons of **a** NH_4^+-N concentrations, **b** NO_3^- -N concentration, **c** NO_2^- -N concentration, **d** N_2O concentration, **e** $\delta^{15}N_{NO_3^-+NO_2^-}$ and **f** $\delta^{18}O_{NO_3^-+NO_2^-}$. The sediments of sites 1 and 2 are sand-dominated and of site 3 are gravel-dominated. The median of the data is indicated by the bold line of the boxplot and the first and third quartiles are shown by the lower and upper hinges

respectively. The smallest value is indicated by the lower whisker while the upper whisker represents the largest value, however, the whiskers do not extend past 1.5* the inter-quartile range of the lower and upper hinges. The individual points are considered outliers as they represent data outside of the range of the whiskers

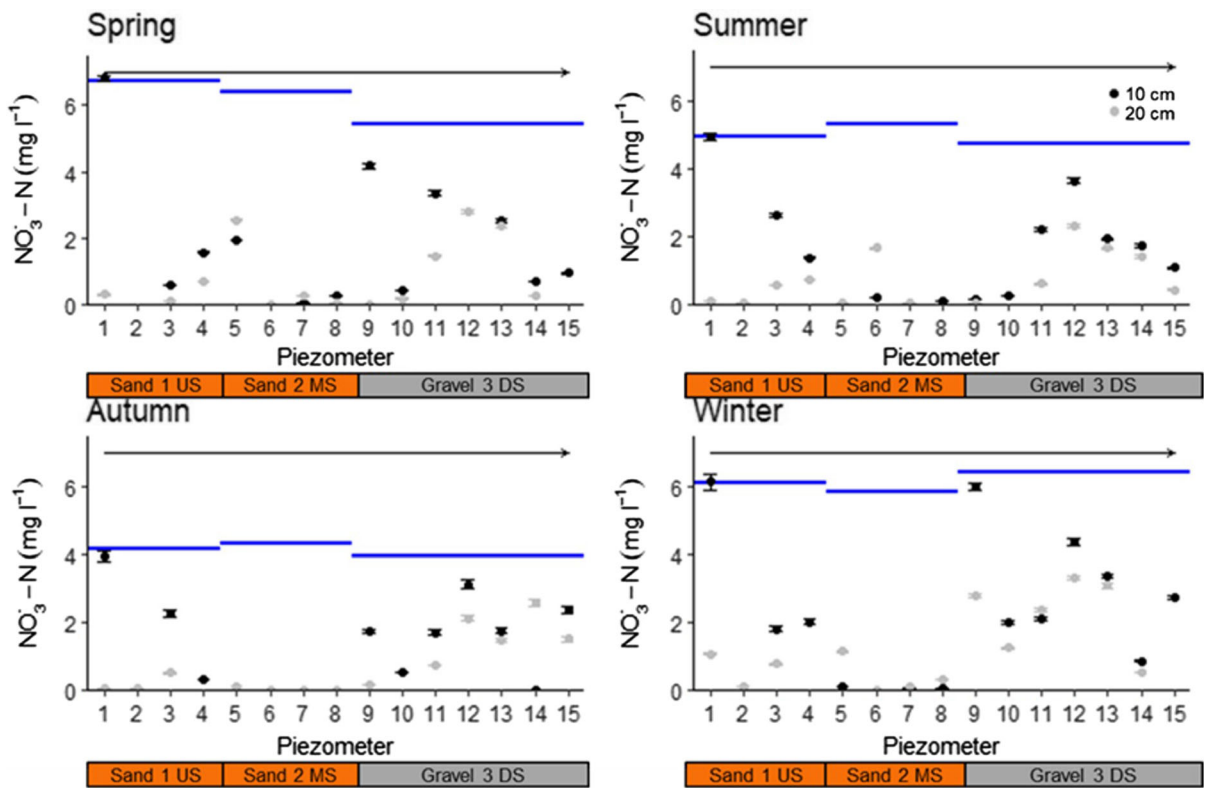


Fig. 3 Porewater NO_3^- -N concentrations at 10 (black) and 20 (grey) cm depth. Surface water concentrations at each site are shown with a blue line and the direction of surface flow from upstream to downstream is indicated with a black arrow

NO_2^-

Porewater NO_2^- concentrations were highest in site 3, with low concentrations found in both sites 1 and 2, which was consistent across all seasons (Fig. 2c), leading to significant differences between sites (p value < 0.001 , Table S4). NO_2^- concentrations varied greatly between seasons in site 3, with concentrations highest in summer and autumn, however, this was not significant (p value > 0.102 , Table S4) and NO_2^- concentrations were higher in the surface water than in the porewaters in sites 1 and 2, but were lower than the porewater concentrations in site 3 in summer, autumn and winter (Fig. S2).

N_2O

Porewater N_2O concentrations were highest in sites 1 and 3, and were significantly different between sites (p value < 0.041 , Table S4), with concentrations in autumn elevated in site 3 compared to site 1 (Fig. 2d).

The seasonal variation in N_2O concentrations was small but significant between autumn and summer (p value = 0.040, Table S4), and concentrations were elevated in autumn in site 3. N_2O concentrations were generally higher in the surface water than in the porewaters in sites 1 and 2, but were lower than the porewater concentrations in site 3 (Fig. 4).

$\delta^{15}\text{N}_{\text{NO}_3^- + \text{NO}_2^-}$ and $\delta^{18}\text{O}_{\text{NO}_3^- + \text{NO}_2^-}$

$\delta^{15}\text{N}_{\text{NO}_3^- + \text{NO}_2^-}$ values in the surface water were similar in all sites and did not vary significantly throughout the year (Fig. S3). Porewater $\delta^{15}\text{N}_{\text{NO}_3^- + \text{NO}_2^-}$ values were generally highest in site 3 resulting in significantly different values between sites (p value < 0.001 , Table S4), which was consistent throughout all seasons, but less pronounced in winter (Fig. 2e). Values varied significantly between autumn and spring, and autumn and winter (p value < 0.008 , Table S4), but were most pronounced at site 3, with lowest ratios found in winter.

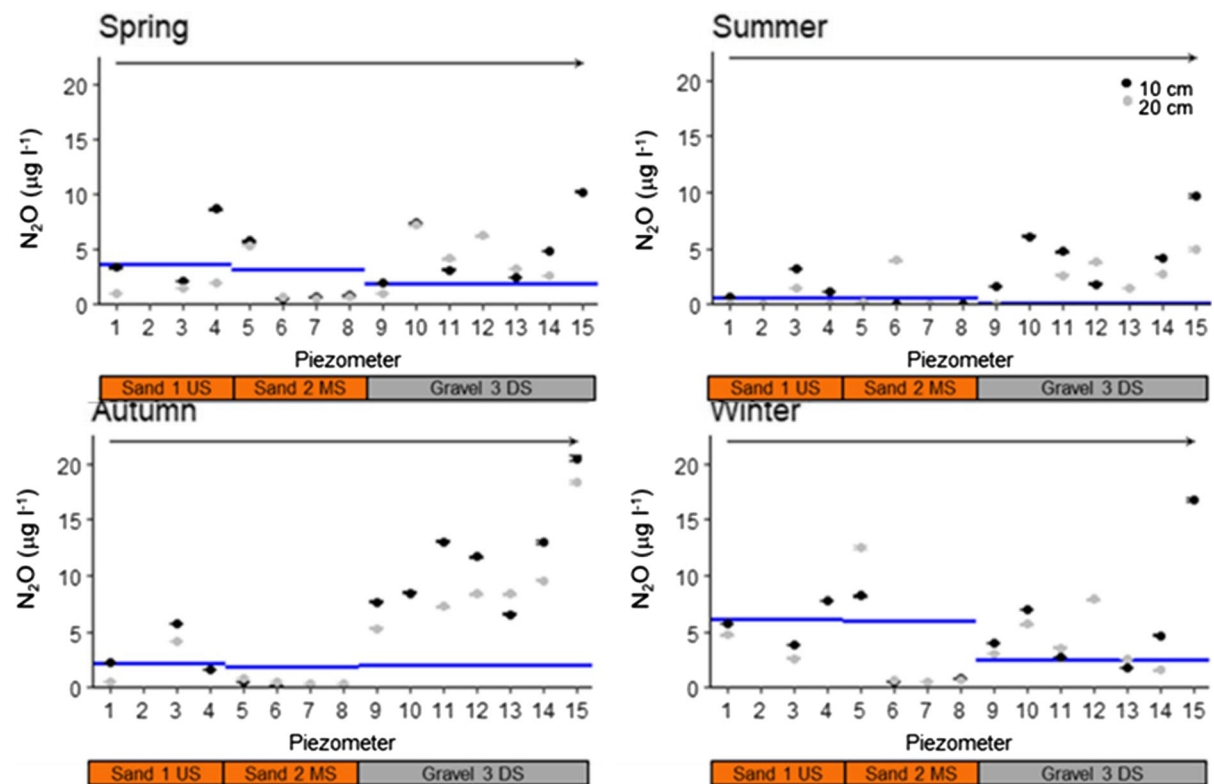


Fig. 4 Porewater N_2O concentrations at 10 (black) and 20 (grey) cm depth. Surface water concentrations at each site are shown with a blue line and the direction of surface flow from upstream to downstream is indicated with a black arrow

$\delta^{18}\text{O}_{\text{NO}_3^- + \text{NO}_2^-}$ values in the surface water were similar in all sites except site 1 in autumn and did not vary greatly throughout the year (Fig. S4). Patterns in porewater $\delta^{18}\text{O}_{\text{NO}_3^- + \text{NO}_2^-}$ values were not very pronounced but were generally lowest in site 1 and highest in site 3 (Fig. 2f). $\delta^{18}\text{O}_{\text{NO}_3^- + \text{NO}_2^-}$ values did not vary greatly with season.

Potential rates of denitrification

Potential rates of denitrification were higher in the sand-dominated than the gravel-dominated across all treatments (Fig. 5). Denitrification potentials in the control experiments, comprising of sediment incubations with no added substrate indicative of conditions within the streambed, were significantly higher (p value = 0.036, Table S3) in the sand-dominated than the gravel-dominated sediments ($0.026 \pm 0.004 \text{ N}_2\text{O-N } \mu\text{g g}^{-1} \text{ h}^{-1}$ for sand-dominated and $0.003 \pm 0.003 \text{ N}_2\text{O-N } \mu\text{g g}^{-1} \text{ h}^{-1}$ for gravel-

dominated). Denitrification potentials in the sand-dominated sediments of the NO_3^- -spiked samples increased to $0.042 \pm 0.025 \text{ N}_2\text{O-N } \mu\text{g g}^{-1} \text{ h}^{-1}$. In the gravel-dominated sediments, the denitrification potential showed no increase over that of the control ($0.003 \pm 0.001 \text{ N}_2\text{O-N } \mu\text{g g}^{-1} \text{ h}^{-1}$), resulting in significantly different denitrification potentials between sediment type (p value = 0.008, Table S3). The addition of C resulted in decreased denitrification potentials in both sediment types ($0.004 \pm 0.004 \text{ N}_2\text{O-N } \mu\text{g g}^{-1} \text{ h}^{-1}$ for sand-dominated and $0.001 \pm 0.001 \text{ N}_2\text{O-N } \mu\text{g g}^{-1} \text{ h}^{-1}$ for gravel-dominated), resulting in no significant differences (p -value = 0.193, Table S3). The mixed substrate experiment, indicative of ideal denitrification conditions with regards to electron donor and acceptor availability, resulted in larger denitrification potentials within the sand-dominated sediment ($0.134 \pm 0.092 \text{ N}_2\text{O-N } \mu\text{g g}^{-1} \text{ h}^{-1}$), which were significantly higher (p value = 0.008, Table S3) than within the gravel-

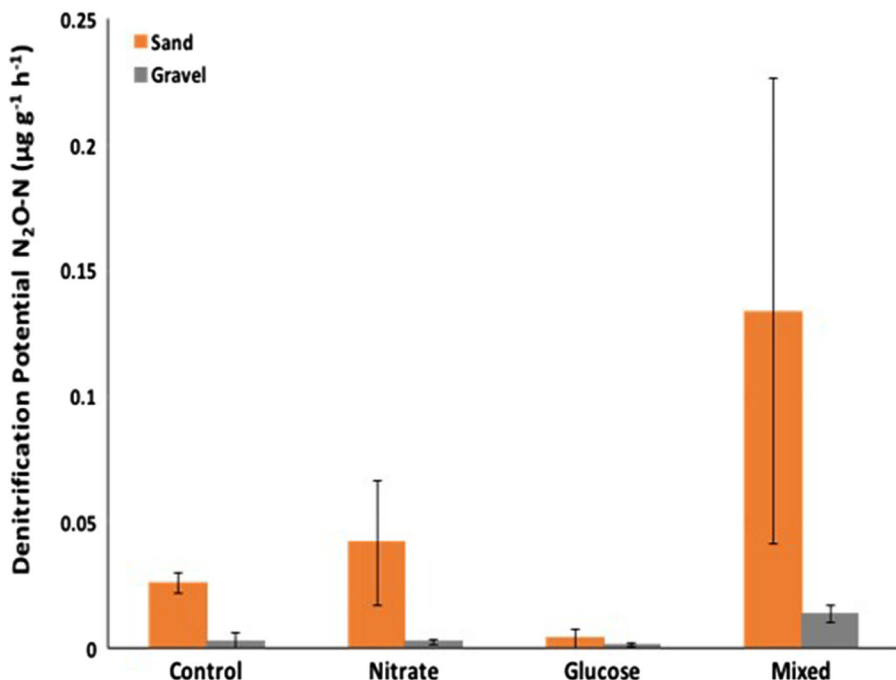


Fig. 5 The potential rate of denitrification of sand and gravel sediments under various conditions, expressed in $\mu\text{g N}_2\text{O-N g}^{-1} \text{h}^{-1}$

dominated sediments ($0.0134 \pm 0.003 \text{ N}_2\text{O N } \mu\text{g g}^{-1} \text{ h}^{-1}$).

The relationship between potential denitrification and N_2O production was calculated as a ratio of potential denitrification from the control experiments to the site-averaged concentration of $\text{N}_2\text{O-N}$ measured in the porewaters at 10 cm depths in summer. The average $\text{N}_2\text{O-N}$ concentration at 10 cm in site 2 was zero so no relationship could be calculated for this depth. The ratio of potential denitrification to $\text{N}_2\text{O-N}$ was 0.048 at site 1 and 0.002 at site 3.

Discussion

N cycling in a wider context

The porewater NO_3^- and N_2O concentrations were typically similar to or lower than those observed previously. The low NO_3^- concentrations in the sand-dominated sediments of site 2 were similar to those found previously in gravel bars of low-order upland streams (e.g. Zarnetske et al. 2011), and the higher concentrations found at sites 1 and 3 were similar or slightly lower than those found in both vegetated and

unvegetated streambed sediments of lowland rivers (Krause et al. 2009; Lansdown et al. 2014, 2015; Ullah et al. 2014). The N_2O concentrations in the sand-dominated sediments of sites 1 and 2 were lower than previously observed in sandy sediments influenced by agriculture (Hinshaw and Dahlgren 2013; Pretty et al. 2006), whereas the concentrations in the gravel-dominated sediments were similar to those found in coarse gravel sediments influenced by agriculture (Pretty et al. 2006), but lower than those found in a gravel bar (Hlaváčová et al. 2005). Together this indicates that nutrient cycling at this study site was similar to or more efficient than that observed in previous studies, attributed to the similar or lower concentrations of NO_3^- and N_2O observed here.

Spatial variation

N cycling and nutrient attenuation were higher, and N_2O concentrations lower, in the sand-dominated sediments than in the gravel-dominated sediments. This is likely due to higher residence times (Table 1) and rates of microbial activity observed in the sand-dominated sediments at this site (Comer-Warner et al. 2019), which is supported by previous observations of

higher residence times in sediments of smaller particle size (Baker et al. 2000). The differences in N cycling between sites may also have been a result of changes in microbial communities and their functional capacities between sites. These factors have been observed to affect methanogenesis in varying sediment types (Crawford et al. 2017). Although no microbial community data exists at the study site, differences in the uptake of recalcitrant carbon observed between the sand- and gravel-dominated sediments at this site suggest differences in the microbial communities (Comer-Warner et al. 2019).

No C limitation of potential denitrification was observed in either the sand- or gravel-dominated sediments, which is likely due to high concentrations ($> 9 \text{ mg C l}^{-1}$) of porewater DOC observed at all three sites (Comer-Warner et al. 2019). This high porewater DOC likely promotes denitrification, affecting NO_3^- concentrations within the streambed, as a direct relationship has been observed between NO_3^- concentration and denitrification rates when DOC concentrations are high (Schade et al. 2016).

The potential of gravel-dominated sediments as a source of N_2O is consistent with previous research, which found significant N_2O production associated with intermediate residence times (Quick et al. 2016). Although nutrient attenuation was highest in the sand-dominated sediments of sites 1 and 2, a decrease in NO_3^- between 10 and 20 cm was observed in most piezometers regardless of site and season (Fig. 3), indicating that surface water NO_3^- was likely attenuated in the sand- and gravel-dominated sediments. NO_3^- concentrations at site 1 were relatively high, suggesting that either nutrient attenuation occurred at a lower level at this site or that NO_3^- inputs were greater at this site. Site 1 received run-off directly from agricultural fields (likely containing high concentrations of NO_3^- from fertiliser) and nitrate isotopes were not more highly enriched at site 1 relative to sites 2 and 3, therefore, the high NO_3^- concentrations observed here are suggested to be due to an increase in NO_3^- inputs at this site, which could counteract the effects of denitrification, maintaining high NO_3^- concentrations.

Seasonal variation

Porewater nitrogen chemistry, including $\delta^{15}\text{N}_{\text{NO}_3^- + \text{NO}_2^-}$ and $\delta^{18}\text{O}_{\text{NO}_3^- + \text{NO}_2^-}$ values, varied seasonally,

particularly in site 3, suggesting an increase in nitrogen cycling, likely through complete and incomplete denitrification (see discussion below), from winter to autumn. The seasonal variation observed could be due to lower microbial activity in winter and spring due to lower temperatures (Lautz and Fanelli 2008), coupled with increased N availability in the stream in autumn due to leaf litter inputs during this time, and higher porewater DOC observed in all sites during summer and autumn (Comer-Warner et al. 2019). Seasonal variations in hydrology would have also affected nitrogen cycling with higher flows and shorter residence times observed in winter and spring limiting denitrification (Nixon et al. 1996). The seasonal variation in N_2O observed here contradicts previous research, which found no significant difference in seasonal N_2O concentrations in streambed gravel sediments (Hlaváčová et al. 2005).

Biogeochemical processes

Relatively high NH_4^+ concentrations in the sand-dominated sediments suggest low rates of nitrification and anammox in this sediment type, which may have also contributed to low concentrations of NO_2^- and N_2O . High denitrification potentials observed in the laboratory experiments, coupled with relatively low concentrations of NO_3^- , NO_2^- and N_2O in the sand-dominated sediments indicate that rates of denitrification were high within these sediments and that the multi-step pathway of denitrification was almost complete. This was further evidenced by isotopic data (see below), as well as the fact that NO_3^- -limitation on denitrification potentials was only observed in the sand-dominated sediments (observed previously at $< 2 \text{ mg NO}_3^- \text{N l}^{-1}$; Schipper and Vojvodić-Vuković 1998).

Conversely, low denitrification potentials coupled with relatively high concentrations of NO_3^- , NO_2^- and N_2O suggest incomplete denitrification within the gravel-dominated sediments. The low NH_4^+ concentrations likely result from high rates of nitrification or the relatively low OM content of the gravel-dominated sediments (Table 1) resulting in less NH_4^+ released from organic matter mineralisation (Duff and Triska 2000). Although anammox may also be present, the high concentrations of NO_2^- and low concentrations of NH_4^+ , respectively, suggest this is a minor process. Isotopic data provide further evidence for

denitrification, coupled with nitrification, as discussed below. The relatively high N_2O in the gravel-dominated sediments, coupled with low C reactivity observed at this site (Comer-Warner et al. 2019), support previous research that N_2O production increases with high NO_3^- and low organic C reactivity (Quick et al. 2016). The differences in denitrification between the two sediment types were further evidenced by the high ratio of potential denitrification to porewater $\text{N}_2\text{O}-\text{N}$ found in site 1 relative to that in site 3, indicating that potential rate and completeness of denitrification is greater in sand- than gravel-dominated sediments. Although incubation experiments to determine potential rates of denitrification showed significant differences between sediment types, acetylene is known to alter microbial community structure on short timescales by up to 9.5% (Fulweiler et al. 2015), which may have affected the resulting denitrification potentials. The potential effect on the results presented here, however, should be small as large differences in potential rates of denitrification between the sediment types were observed. Additionally, acetylene may reduce N_2O production resulting in underestimation of potential rates of denitrification (Bollmann and Conrad 1997; Felber et al. 2012; Nadeem et al. 2013).

The suggestion that the nitrogen patterns observed here are predominantly due to complete and incomplete denitrification, with nitrification also an important process in the gravel-dominated sediments, is further evidenced by the patterns of in-situ isotopic data observed. Previous research has also indicated that denitrification and nitrification are the dominant N-cycling processes in streambed sediments (Bollmann and Conrad 1998; Davidson 1991; Heppell et al. 2013; Lansdown et al. 2012, 2015; Quick et al. 2016; Well et al. 2005), however, it should be noted that anammox has been found to occur at higher rates than denitrification in oxic, permeable riverbeds (Lansdown et al. 2016). We infer from the nitrate isotope data that nitrogen cycling is likely due to denitrification, therefore, although the reactions resulting in the high NO_2^- , and N_2O concentrations have not been determined as we do not have information on rates of the other processes involved in nitrogen cycling, it follows that these are also due to denitrification.

The $\delta^{15}\text{N}_{\text{NO}_3^-+\text{NO}_2^-}$ and $\delta^{18}\text{O}_{\text{NO}_3^-+\text{NO}_2^-}$ values observed in the surface water were consistently similar

between sites and seasons, except in site 1 in autumn, which had a slightly higher $\delta^{18}\text{O}_{\text{NO}_3^-+\text{NO}_2^-}$ value. This suggests that the source of NO_3^- and the processes affecting NO_3^- concentrations were not significantly different in the surface water between site and season, therefore, most differences in nitrate isotopes were likely process-driven with the processes affecting NO_3^- concentrations occurring within the sediments. The high values of $\delta^{15}\text{N}_{\text{NO}_3^-+\text{NO}_2^-}$ and $\delta^{18}\text{O}_{\text{NO}_3^-+\text{NO}_2^-}$ observed at all three sites, combined with $\delta^{15}\text{N}:\delta^{18}\text{O}$ ratios from site-averaged porewater samples typically between 2.1 and 2.5 and a linear relationship between $\delta^{15}\text{N}_{\text{NO}_3^-+\text{NO}_2^-}$ and $\delta^{18}\text{O}_{\text{NO}_3^-+\text{NO}_2^-}$ (Fig. 6) indicate that denitrification was the dominant process here (Amberger and Schmidt 1987; Kendall 1998; Granger and Wankel 2016). Various processes may affect nitrate isotopes, however, which alter the observed slope of $\delta^{15}\text{N}:\delta^{18}\text{O}$ ratios, with slopes < 1 indicating isotopic overprinting of nitrification, and slopes > 1 indicating isotopic overprinting of anammox (Granger and Wankel 2016). This suggests that nitrification, and not anammox, was also occurring in the porewaters here, as supported by the concentration data discussed above. A summary of the suggested processes and resulting dominant N species is presented in Fig. 7. It should be noted, however, that the diagrams in Fig. 6 are based on global data from the literature; it is necessary to fully characterise the isotopic values of local sources to accurately interpret source and process information. In addition, the differences in slopes caused by isotopic overprinting were determined assuming the slope of $\delta^{15}\text{N}:\delta^{18}\text{O}$ ratios for denitrification is 1 (Granger and Wankel 2016).

Surprisingly, given the indication from the potential rates of denitrification and porewater concentrations that denitrification was highest in the sand-dominated sediments, the $\delta^{15}\text{N}_{\text{NO}_3^-+\text{NO}_2^-}$ and $\delta^{18}\text{O}_{\text{NO}_3^-+\text{NO}_2^-}$ values were higher in the gravel-dominated sediments suggesting relatively high rates of denitrification. One explanation for this is that denitrification had progressed to completion or almost completion in the sand-dominated sediments and so the isotopes were no longer enriched relative to the signal produced by the incomplete denitrification occurring in the gravel-dominated sediments. It is possible, however, that the gravel-dominated sediments of site 3, which were typically characterised by

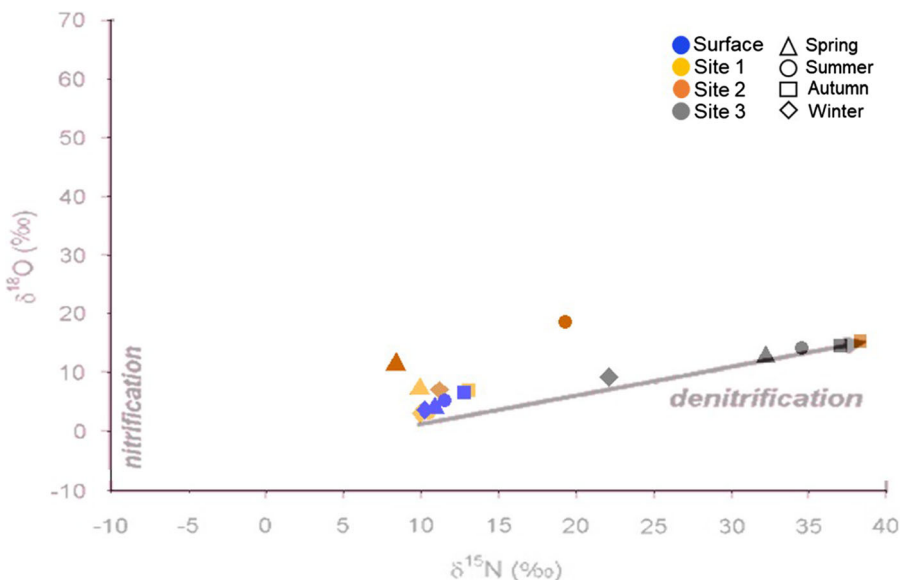


Fig. 6 Average porewater isotopic ratios per site from the multilevel piezometers, as well as surface water isotopic ratios, plotted onto a modified ‘Kendall diagram’ of typical global

isotopic ratios resulting from nitrification and denitrification. The arrow represents a theoretical ratio of dual isotopic enrichment due to denitrification (Kendall 1998)

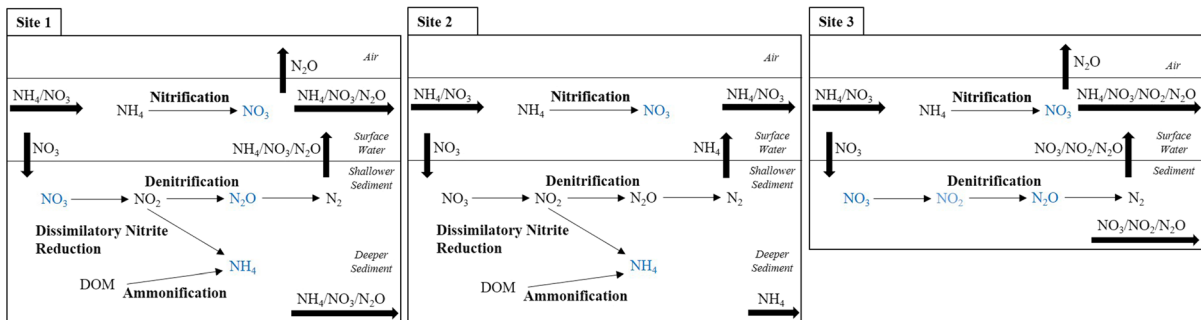


Fig. 7 A conceptual figure of the processes occurring in the surface water and porewaters of the three study sites. Nitrogen species are shown in blue where they occurred at high

concentrations, processes are represented by ‘thin’ arrows and labelled in bold, and transportation is represented by ‘thick’ arrows. (Color figure online)

higher subsurface fluxes (Table 1), received a different subsurface input of isotopically-enriched NO_3^- .

Interestingly, in-situ measurements from the sand-dominated sites, which were characterised by the highest potential rates of denitrification, provided the lowest concentrations of N_2O and isotopic values of NO_3^- and therefore, the gravel-dominated site with incomplete denitrification provided the clearest evidence for denitrification. This is likely due to denitrification progressing to completion or almost completion in the sand-dominated sediments,

therefore, this may suggest there are limitations in using field measurements to detect denitrification as the clearest evidence of complete denitrification is the same as no denitrification.

The denitrifier method used in the isotopic analysis measures $\delta^{15}\text{N}_{\text{NO}_3^- + \text{NO}_2^-}$ and $\delta^{18}\text{O}_{\text{NO}_3^- + \text{NO}_2^-}$ in both NO_3^- and NO_2^- (Casciotti et al. 2002; Sigman et al. 2001), therefore, samples in which the ratio of $\text{NO}_2^- : \text{NO}_3^-$ was high may be influenced by $\delta^{15}\text{N}_{\text{NO}_2^-}$. Samples where the concentration of NO_2^- was higher than 5% of the concentration of NO_3^- were found in

some piezometers (Table S5). These samples accounted for many of the extreme values of $\delta^{15}\text{N}_{\text{NO}_3^- + \text{NO}_2^-}$ observed, and although the remaining samples also had higher $\delta^{15}\text{N}_{\text{NO}_3^- + \text{NO}_2^-}$ values in the porewaters of site 3, the difference between the sand-dominated and gravel-dominated sediments was greatly reduced. Investigations of NO_2^- isotopes during nitrogen cycling have shown that NO_2^- oxidation to NO_3^- during nitrification results in both $\delta^{15}\text{N}_{\text{NO}_2^-}$ and $\delta^{18}\text{O}_{\text{NO}_2^-}$ being depleted, whereas during microbial NO_2^- reduction in denitrification both $\delta^{15}\text{N}_{\text{NO}_2^-}$ and $\delta^{18}\text{O}_{\text{NO}_2^-}$ are enriched (Buchwald et al. 2012; Casciotti 2009; Martin and Casciotti 2016). Given that our isotopic data indicates that denitrification is the dominant process occurring at the study site, samples with high NO_2^- concentrations are expected to be relatively enriched in $\delta^{15}\text{N}_{\text{NO}_3^- + \text{NO}_2^-}$ and $\delta^{18}\text{O}_{\text{NO}_3^- + \text{NO}_2^-}$, explaining why the samples high in NO_2^- also tended to have higher $\delta^{15}\text{N}_{\text{NO}_3^- + \text{NO}_2^-}$ and $\delta^{18}\text{O}_{\text{NO}_3^- + \text{NO}_2^-}$ values.

Although the evidence suggests that the differences in complete and incomplete denitrification and N_2O concentrations observed here between sediment types are due to differences in residence times observed between the sand-dominated and gravel-dominated sediments (Table 1), it is possible that denitrification occurred at greater depths in the gravel-dominated sediments and so was not fully captured by the maximum sampling depth of 20 cm used in this study. Furthermore, N_2O concentrations in the surface water were generally higher above the sand-dominated sediments than the gravel-dominated sediments. This does not, however, necessarily indicate a higher N_2O flux into the surface water from the sand-dominated sediments because of the dynamic nature of N_2O concentrations in surface water, which are affected by outgassing and transport.

The control of sediment type on potential denitrification and concentrations of N species was observed here in an agricultural stream abundant in DOC. Results presented here, therefore, may not be broadly applicable beyond this type of stream. Further work determining N_2O fluxes out of the streambed is required to confirm their importance, as well as the generality of findings to streams with varying land-use and DOC availability.

Additionally, future work to fully constrain the drivers of nutrient consumption and N_2O production within streambed sediments, and subsequent contributions to atmospheric fluxes, is required. This is especially crucial given the estimated importance of agricultural streams and rivers in the global N_2O cycle, and predictions that N_2O fluxes will increase in the future due to increased nutrient loading and temperature, and changes in land use (Venkiteswaran et al. 2014). Furthermore, future work across multiple sites of contrasting sediment types is necessary to further consolidate understanding of the differences in N cycling between sediment type.

Conclusions

N cycling in the investigated agricultural lowland stream was strongly controlled by sediment type, with sand-dominated sediments characterised by higher rates of denitrification than gravel-dominated sediments. This resulted in incomplete denitrification and associated high concentrations of N_2O at 10 and 20 cm, in the gravel-dominated sediments. Our results, therefore, indicate that NO_3^- reduction is highest in sand-dominated sediments, however, production of the GHG, N_2O , is highest in gravel-dominated sediments. Additionally, we identified significant seasonal variability in complete and incomplete denitrification, with rates increasing from winter to autumn.

Acknowledgments The authors would like to thank the Birmingham Institute of Forest Research for their support and use of the study site, Anika Comer-Warner for her role as a field assistant and Dr. Ben Marchant for his advice on the statistical analysis. We would also like to thank NERC for their financial support through a Central England NERC Training Alliance Studentship and the Grant NE/L004437/1, as well as the European Union who provided funding via the H2020-MSCA-RISE-2016 Project 734317. The data supporting the conclusions in this manuscript can be found in NERC's Environmental Information Data Centre, <https://doi.org/10.5285/00601260-285e-4ffa-b381-340b51a7ec50>, title: Seasonal streambed carbon and nitrogen cycling (including greenhouse gases) in an agriculturally-impacted stream. Measured at Wood Brook UK, 2016–2017 and <https://doi.org/10.5285/500193f7-2653-4696-8224-276a734ed6ab>, title: Rates of fluorescein diacetate hydrolysis, phenol oxidation and potential denitrification in sand and gravel sediments from an agriculturally-impacted stream.

Open Access This article is licensed under a Creative Commons Attribution 4.0 International License, which permits use,

sharing, adaptation, distribution and reproduction in any medium or format, as long as you give appropriate credit to the original author(s) and the source, provide a link to the Creative Commons licence, and indicate if changes were made. The images or other third party material in this article are included in the article's Creative Commons licence, unless indicated otherwise in a credit line to the material. If material is not included in the article's Creative Commons licence and your intended use is not permitted by statutory regulation or exceeds the permitted use, you will need to obtain permission directly from the copyright holder. To view a copy of this licence, visit <http://creativecommons.org/licenses/by/4.0/>.

References

Alexander RB, Smith RA, Schwarz GE (2000) Effect of stream channel size on the delivery of nitrogen to the Gulf of Mexico. *Nature* 403:758–761

Allen G, Pavelsky T (2018) Global extent of rivers and streams. *Science*. <https://doi.org/10.5268/IW-2.4.502>

Amberger A, Schmidt H-L (1987) Naturliche Isotopengehalte von Nitrat als Indikatoren fur dessen Herkunft. *Geochim Cosmochim Acta* 51:2699–2705

Anderson B, Bartlett K, Frolking S, Hayhoe K, Jenkins J, Salas WA (2010) Methane and nitrous oxide emissions from natural sources. Office of Atmospheric Programs, US EPA, EPA 430-R-10-001, Washington, DC. https://scholar.google.com/scholar?q=EPA+%282010%29.+Methane+and+Nitrous+Oxide+Emissions+from+Natural+Sources+&btnG=&hl=en&as_sdt=0%2C33#

Baker MA, Dahm CN, Valett HM (2000) Anoxia, anaerobic metabolism, and biogeochemistry of the stream-groundwater interface. In: Jones JB, Mulholland PJ (eds) Streams and ground waters, 2nd edn. Elsevier, San Diego, pp 259–283

Bakken LR, Bergaust L, Liu B, Frostegard A (2012) Regulation of denitrification at the cellular level: a clue to the understanding of N₂O emissions from soils. *Philosoph Trans R Soc B* 367(1593):1226–1234. <https://doi.org/10.1098/rstb.2011.0321>

Beaulieu JJ, Tank JL, Hamilton SK, Wollheim WM, Hall RO, Mulholland PJ et al (2011) Nitrous oxide emission from denitrification in stream and river networks. *Proc Natl Acad Sci* 108(1):214–219. <https://doi.org/10.1073/pnas.1011464108>

Blaen PJ, Khamis K, Lloyd C, Comer-Warner S, Ciocca F, Thomas RM et al (2017) High-frequency monitoring of catchment nutrient exports reveals highly variable storm event responses and dynamic source zone activation. *J Geophys Res* 122:1–17. <https://doi.org/10.1002/2017JG003904>

Böhlke JK, Mroczkowski SJ, Coplen TB (2003) Oxygen isotopes in nitrate: new reference materials for 18O:17O:16O measurements and observations on nitrate-water equilibration. *Rapid Commun Mass Spectrom* 17:1835–1846. <https://doi.org/10.1002/rcm.1123>

Bollmann A, Conrad R (1997) Acetylene blockage technique leads to underestimation of denitrification rates in oxic soils due to scavenging of intermediate nitric oxide. *Soil Biol Biochem* 29(7):1067–1077

Bollmann A, Conrad R (1998) Influence of O₂ availability on NO and N₂O release by nitrification and denitrification in soils. *Glob Change Biol* 4(4):387–396. <https://doi.org/10.1046/j.1365-2486.1998.00161.x>

Bonin P, Tamburini C, Michotey V (2002) Determination of the bacterial processes which are sources of nitrous oxide production in marine samples. *Water Res* 36(3):722–732. [https://doi.org/10.1016/S0043-1354\(01\)00269-X](https://doi.org/10.1016/S0043-1354(01)00269-X)

Boulton AJ, Findlay S, Marmonier P, Stanley EH, Valett HM (1998) The functional significance of the hyporheic zone in streams and rivers. *Annu Rev Ecol Syst* 29:59–81. <https://doi.org/10.1146/annurev.ecolsys.29.1.59>

Brunke M, Gonser T (1997) The ecological significance of exchange processes between rivers and groundwater. *Freshw Biol* 37(1):1–33. <https://doi.org/10.1046/j.1365-2427.1997.00143.x>

Buchwald C, Santoro AE, McIlvin MR, Casciotti KL (2012) Oxygen isotopic composition of nitrate and nitrite produced by nitrifying cocultures and natural marine assemblages. *Limnol Oceanogr* 57(5):1361–1375. <https://doi.org/10.4319/lo.2012.57.5.1361>

Burgin AJ, Lazar JG, Grossman PM, Gold AJ, Kellogg DQ (2013) Balancing nitrogen retention ecosystem services and greenhouse gas disservices at the landscape scale. *Ecol Eng* 56:26–35. <https://doi.org/10.1016/j.ecoleng.2012.05.003>

Casciotti KL (2009) Inverse kinetic isotope fractionation during bacterial nitrite oxidation. *Geochim Cosmochim Acta* 73:2061–2076. <https://doi.org/10.1016/j.gca.2008.12.022>

Casciotti KL, Sigman DM, Hastings MG, Bohlke JK, Hilkert A (2002) Measurement of the oxygen isotopic composition of nitrate in seawater and freshwater using the dentirifier method. *Anal Chem* 74:4905–4912

Codispoti LA (2010) Interesting Times for Marine N₂O. *Science* 327:1339–1340

Comer-Warner SA, Goody DC, Ullah S, Glover L, Percival A, Kettridge N, Krause S (2019) Seasonal variability of sediment controls of carbon cycling in an agricultural stream. *Sci Total Environ* 688:732–741. <https://doi.org/10.1016/j.scitotenv.2019.06.317>

Crawford JT, Loken LC, West WE, Crary B, Spahn SA, Gubbins N et al (2017) Spatial heterogeneity of within-stream methane concentrations. *J Geophys Res* 122:1036–1048. <https://doi.org/10.1002/2016JG003698>

Davidson EA (1991) Fluxes of nitrous oxide and nitric oxide from terrestrial ecosystems. In: Rogers JE, Whitman WB (eds) Microbial production and consumption of greenhouse gases: methane, nitrogen oxides, and halomethanes. American Society for Microbiology, Washington, DC, pp 219–235

Duff JH, Triska FJ (2000) Nitrogen biogeochemistry and surface-subsurface exchange in streams. In: Jones J, Mulholland PJ (eds) Streams and ground waters, 2nd edn. Elsevier Inc, San Diego, pp 197–220

Duff JH, Tesoriero AJ, Richardson WB, Strauss EA, Munn MD (2008) Whole-stream response to nitrate loading in three streams draining agricultural landscapes. *J Environ Qual* 37(3):1133. <https://doi.org/10.2134/jeq2007.0187>

Felber R, Conen F, Flechard CR, Neftel A (2012) Theoretical and practical limitations of the acetylene inhibition technique to determine total denitrification losses. *Biogeoosciences* 9:4125–4138. <https://doi.org/10.5194/bg-9-4125-2012>

Findlay S (1995) Importance of surface-subsurface exchange in stream ecosystems: the hyporheic zone. *Limnol Oceanogr* 40(1):159–164. <https://doi.org/10.4319/lo.1995.40.1.0159>

Findlay SEG, Mulholland PJ, Hamilton SK, Tank JL, Bernot MJ, Burgin AJ et al (2011) Cross-stream comparison of substrate-specific denitrification potential. *Biogeochemistry* 104:381–392. <https://doi.org/10.1007/s10533-010-9512-8>

Forster P, Ramaswamy V, Artaxo P, Berntsen T, Betts R, Fahey DW et al. (2007) Changes in atmospheric constituents and in radiative forcing. In: S Solomon, D Qin, M Manning, Z Chen, M Marquis, K Averyt et al. (eds) Climate change 2007: the physical science basis. Contribution of Working Group I to the Fourth Assessment Report of the Intergovernmental Panel on Climate Change. Cambridge University Press, Cambridge

Fulweiler RW, Heiss EM, Rogener MK, Newell SE, LeCleir GR, Kortbein SM, Wilhelm SW (2015) Examining the impact of acetylene on N-fixation and the active sediment microbial community. *Frontiers Microbiol* 6:418. <https://doi.org/10.3389/fmicb.2015.00418>

García-Ruiz R, Pattinson SN, Whitton BA (1998) Denitrification and nitrous oxide production in sediments of the Wiske, a lowland eutrophic river. *Sci Total Environ* 210(211):307–320

Glibert P, Seitzinger S, Heil C, Burkholder J, Parrow M, Codispoti L, Kelly V (2005) The role of eutrophication in the global proliferation of harmful algal blooms. *Oceanography* 18(2):198–209. <https://doi.org/10.5670/oceanog.2005.54>

Gomez-Velez JD, Harvey JW, Cardenas MB, Kiel B (2015) Denitrification in the Mississippi River network controlled by flow through river bedforms. *Nat Geosci*. <https://doi.org/10.1038/ngeo2567>

Granger J, Wankel SD (2016) Isotopic overprinting of nitrification on denitrification as a ubiquitous and unifying feature of environmental nitrogen cycling. *PNAS* 113(42):E6391–E6400. <https://doi.org/10.1073/pnas.1601383113>

Grimm NB, Fisher SG (1984) Exchange between interstitial and surface water: implications for stream metabolism and nutrient cycling. *Hydrobiologia* 111(3):219–228. <https://doi.org/10.1007/BF00007202>

Heppell C, Louise-Heathwaite A, Binley A, Byrne P, Ullah S, Lansdown K et al (2013) Interpreting spatial patterns in redox and coupled water–nitrogen fluxes in the streambed of a gaining river reach. *Biogeochemistry* 117(2–3):491–509. <https://doi.org/10.1007/s10533-013-9895-4>

Hinshaw SE, Dahlgren RA (2013) Dissolved nitrous oxide concentrations and fluxes from the Eutrophic San Joaquin River, California. *Environ Sci Technol* 47:1313–1322

Hlaváčová E, Rulík M, Čáp L (2005) Anaerobic microbial metabolism in hyporheic sediment of a gravel bar in a small lowland stream. *River Res Appl* 21(9):1003–1011. <https://doi.org/10.1002/rra.866>

Hudson, F. (2004). *Sample Preparation and Calculations for Dissolved Gas Analysis in Water Samples Using a GC Headspace Equilibration Technique*. <https://archive.epa.gov/region1/info/testmethods/web/pdf/rsksp175v2.pdf>

Kaiser J, Hastings MG, Houlton BZ, Ro T, Sigman DM (2007) Triple oxygen isotope analysis of nitrate using the denitrifier method and thermal decomposition of N₂O. *Anal Chem* 79(2):599–607. <https://doi.org/10.1021/ac0256282>

Kaplan LA, Newbold JD (2000) Surface and subsurface dissolved organic carbon. In: Jones JB, Mulholland PJ (eds) Streams and ground waters. Elsevier Inc, San Diego, pp 237–253

Kelso BHL, Smith RV, Laughlin RJ, Lennox SD (1997) Dissimilatory nitrate reduction in anaerobic sediments leading to river nitrite accumulation. *Appl Environ Microbiol* 63(12):4679–4685

Kemp WM, Boynton WR, Adolf JE, Boesch DF, Boicourt WC, Brush G et al (2005) Eutrophication of Chesapeake Bay: historical trends and ecological interactions. *Mar Ecol Prog Ser* 303:1–29. <https://doi.org/10.3354/meps303001>

Kendall, C. (1998). Tracing Nitrogen sources and cycling in catchments. In: Isotope tracers in catchment hydrology, pp 519–576.

Krause S, Heathwaite L, Binley A, Keenan P (2009) Nitrate concentration changes at the groundwater-surface water interface of a small Cumbrian river. *Hydrol Process* 23:2195–2211. <https://doi.org/10.1002/hyp>

Krause S, Tecklenburg C, Munz M, Naden E (2013) Streambed nitrogen cycling beyond the hyporheic zone: flow controls on horizontal patterns and depth distribution of nitrate and dissolved oxygen in the upwelling groundwater of a lowland river. *J Geophys Res* 118(1):54–67. <https://doi.org/10.1029/2012JG002122>

Lansdown K, Trimmer M, Heppell CM, Sgouridis F, Ullah S, Heathwaite AL et al (2012) Characterization of the key pathways of dissimilatory nitrate reduction and their response to complex organic substrates in hyporheic sediments. *Limnol Oceanogr* 57(2):387–400. <https://doi.org/10.4319/lo.2012.57.2.0387>

Lansdown K, Heppell CM, Dossena M, Ullah S, Heathwaite AL, Binley A et al (2014) Fine-scale in situ measurement of riverbed nitrate production and consumption in an armored permeable riverbed. *Environ Sci Technol* 48(8):4425–4434. <https://doi.org/10.1021/es4056005>

Lansdown K, Heppell CM, Trimmer M, Binley A, Heathwaite AL, Byrne P, Zhang H (2015) The interplay between transport and reaction rates as controls on nitrate attenuation in permeable, streambed sediments. *J Geophys Res* 120(6):1093–1109. <https://doi.org/10.1002/2014JG002874>

Lansdown K, McKew BA, Whitby C, Heppell CM, Dumbrell AJ, Binley A et al (2016) Importance and controls of anaerobic ammonium oxidation influenced by riverbed geology. *Nat Geosci* 9:357–360. <https://doi.org/10.1038/ngeo2684>

Lautz LK, Fanelli RM (2008) Seasonal biogeochemical hotspots in the streambed around restoration structures. *Biogeochemistry* 91:85–104. <https://doi.org/10.1007/s10533-008-9235-2>

Martin TS, Casciotti KL (2016) Nitrogen and oxygen isotopic fractionation during microbial nitrite reduction. *Limnol*

Oceanogr 61:1134–1143. <https://doi.org/10.1002/ino.10278>

McAuliffe C (1971) Gas chromatographic determination of solutes by multiple phase equilibrium. *Chem Technol* 1:46–51

McClain ME, Boyer EW, Dent CL, Gergel SE, Grimm NB, Groffman PM et al (2003) Biogeochemical hot spots and hot moments at the interface of terrestrial and aquatic ecosystems. *Ecosystems* 6(4):301–312. <https://doi.org/10.1007/s10021-003-0161-9>

McMahon PB, Böhlke JK (1996) Denitrification and mixing in a stream-aquifer system: effects on nitrate loading to surface water. *J Hydrol* 186(1–4):105–128. [https://doi.org/10.1016/S0022-1694\(96\)03037-5](https://doi.org/10.1016/S0022-1694(96)03037-5)

Mosier A, Kroeze C, Nevison C, Oenema O, Seitzinger S (1998) Closing the global N₂O budget: nitrous oxide emissions through the agricultural nitrogen cycle inventory methodology. *Nutr Cycl Agroecosyst* 52(2–3):225–248. <https://doi.org/10.1023/A:1009740530221>

Mulholland PJ, Tank JL, Sanzone DM, Wollheim W, Peterson BJ, Webster JR et al (2000) Nitrogen cycling in a forest stream determined by a ¹⁵N tracer addition. *Ecol Monogr* 70(3):471–493

Mulholland PJ, Helton AM, Poole GC, Hall RO, Hamilton SK, Peterson BJ et al (2008) Stream denitrification across biomes and its response to anthropogenic nitrate loading. *Nature* 452(7184):202–205. <https://doi.org/10.1038/nature06686>

Nadeem S, Dörsch P, Bakken LR (2013) Autoxidation and acetylene-accelerated oxidation of NO in a 2-phase system: implications for the expression of denitrification in ex situ experiments. *Soil Biol Biochem* 57:606–614. <https://doi.org/10.1016/j.soilbio.2012.10.007>

Nixon SW, Ammerman JW, Atkinson LP, Berounsky VM, Billen G, Boicourt WC et al (1996) The fate of nitrogen and phosphorus at the land-sea margin of the North Atlantic Ocean. *Biogeochemistry* 35:141–180

Pinay G, O'Keefe T, Edwards R, Naiman R (2009) Nitrate removal in the hyporheic zone of a salmon river in Alaska. *River Res Appl* 25:367–375. <https://doi.org/10.1002/rra>

Pinay G, Peiffer S, De Dreuzy JR, Krause S, Hannah DM, Fleckenstein JH et al (2015) Upscaling nitrogen removal capacity from local hotspots to low stream orders' Drainage Basins. *Ecosystems* 18:1101–1120. <https://doi.org/10.1007/s10021-015-9878-5>

Pinay G, Bernal S, Abbott BW, Lupon A, Martí E, Sabater F, Krause S (2018) Riparian corridors: a new conceptual framework for assessing nitrogen buffering across biomes. *Frontiers Environ Sci* 6:47. <https://doi.org/10.3389/FENVS.2018.00047>

Pinheiro J, Bates D, DebRoy S, Sarkar D, R Core Team (2017) nlme: linear and nonlinear mixed effects models. <https://CRAN.R-project.org/package=nlme>.

Pretty JL, Hildrew AG, Trimmer M (2006) Nutrient dynamics in relation to surface–subsurface hydrological exchange in a groundwater fed chalk stream. *J Hydrol* 330(1–2):84–100. <https://doi.org/10.1016/j.jhydrol.2006.04.013>

Quick AM, Reeder WJ, Farrell TB, Tonina D, Feris KP, Benner SG (2016) Controls on nitrous oxide emissions from the hyporheic zones of streams. *Environ Sci Technol*. <https://doi.org/10.1021/acs.est.6b02680>

Quick AM, Reeder WJ, Farrell TB, Tonina D, Feris KP, Benner SG (2019) Nitrous oxide from streams and rivers: a review of primary biogeochemical pathways and environmental variables. *Earth Sci Rev* 191:224–262. <https://doi.org/10.1016/j.earscirev.2019.02.021>

Ravishankara AR, Daniel JS, Portmann RW (2009) Nitrous oxide (N₂O): the dominant ozone-depleting substance emitted in the 21st century. *Science* 326:123–125. <https://doi.org/10.1126/science.1176985>

Rivett MO, Ellis PA, Greswell RB, Ward RS, Roche RS, Cleverly MG et al (2008a) Cost-effective mini drive-point piezometers and multilevel samplers for monitoring the hyporheic zone. *Q J Eng Geol Hydrogeol* 41(1):49–60. <https://doi.org/10.1144/1470-9236/07-012>

Rivett MO, Buss SR, Morgan P, Smith JWN, Bemment CD (2008b) Nitrate attenuation in groundwater: a review of biogeochemical controlling processes. *Water Res* 42(16):4215–4232. <https://doi.org/10.1016/j.watres.2008.07.020>

Schade JD, Bailio J, McDowell WH (2016) Greenhouse gas flux from headwater streams in New Hampshire, USA: patterns and drivers. *Limnol Oceanogr* 61:S165–174. <https://doi.org/10.1002/ino.10337>

Schipper L, Vojvodić-Vuković M (1998) Nitrate removal from groundwater using a denitrification wall amended with sawdust: field trial. *J Environ Qual* 27:664. <https://doi.org/10.2134/jeq1998.00472425002700030025x>

Seitzinger SP, Kroeze C, Bouwman AF, Caraco N, Dentener F, Styles RV (2002) Global patterns of dissolved inorganic and particulate nitrogen inputs to coastal systems: recent conditions and future projections. *Estuaries* 25(4b):640–655

Senbayram M, Chen R, Budai A, Bakken L, Dittter K (2012) N₂O emission and the N₂O/(N₂O+N₂) product ratio of denitrification as controlled by available carbon substrates and nitrate concentrations. *Agr Ecosyst Environ* 147(1):4–12. <https://doi.org/10.1016/j.agee.2011.06.022>

Sgouridis F, Ullah S (2014) Denitrification potential of organic, forest and grassland soils in the Ribble-Wyre and Conwy River catchments, UK. *Environ Sci* 16:1551–1562. <https://doi.org/10.1039/C3EM00693J>

Shelley F, Klaar M, Krause S, Trimmer M (2017) Enhanced hyporheic exchange flow around woody debris does not increase nitrate reduction in sandy streambed. *Biogeochemistry* 136(3):1–20

Sigman DM, Casciotti KL, Andreani M, Barford C, Galanter M, Bohlke JK (2001) A bacterial method for the nitrogen isotopic analysis of nitrate in seawater and freshwater. *Anal Chem* 73(17):4145–4153

Silvennoinen H, Liikanen A, Torssonen J, Stange CF, Martikainen PJ (2008a) Denitrification and N₂O effluxes in the Bothnian Bay (northern Baltic Sea) river sediments as affected by temperature under different oxygen concentrations. *Biogeochemistry* 88(1):63–72. <https://doi.org/10.1007/s10533-008-9194-7>

Silvennoinen H, Liikanen A, Torssonen J, Florian Stange C, Martikainen PJ (2008b) Denitrification and nitrous oxide effluxes in boreal, eutrophic river sediments under increasing nitrate load: a laboratory microcosm study. *Biogeochemistry* 91(2–3):105–116. <https://doi.org/10.1007/s10533-008-9262-z>

Smith VH, Tilman GD, Nekola JC (1999) Eutrophication: impacts of excess nutrient inputs on freshwater, marine, and terrestrial ecosystems. *Environ Pollut* 100:179–196. [https://doi.org/10.1016/S0269-7491\(99\)00091-3](https://doi.org/10.1016/S0269-7491(99)00091-3)

Sophocleous M (2002) Interactions between groundwater and surface water: the state of the science. *Hydrogeol J* 10(1):52–67. <https://doi.org/10.1007/s10040-001-0170-8>

Stevens RJ, Laughlin RJ (1998) Measurement of nitrous oxide and di-nitrogen emissions from agricultural soils. *Nutr Cycl Agroecosyst* 52:131–139. <https://doi.org/10.1023/A:1009715807023>

Trimmer M, Grey J, Heppell CM, Hildrew AG, Lansdown K, Stahl H, Yvon-Durocher G (2012) River bed carbon and nitrogen cycling: state of play and some new directions. *Sci Total Environ* 434:143–158. <https://doi.org/10.1016/j.scitotenv.2011.10.074>

Ullah S, Zhang H, Heathwaite AL, Heppell C, Lansdown K, Binley A, Trimmer M (2014) Influence of emergent vegetation on nitrate cycling in sediments of a groundwater-fed river. *Biogeochemistry* 118(1–3):121–134. <https://doi.org/10.1007/s10533-013-9909-2>

Venkiteswaran JJ, Rosamond MS, Schiff SL (2014) Nonlinear response of riverine N₂O fluxes to oxygen and temperature. *Environ Sci Technol* 48(3):1566–1573. <https://doi.org/10.1021/es500069j>

Venkiteswaran JJ, Boeckx P, Gooddy DC (2019) Towards a global interpretation of dual nitrate isotopes in surface waters. *J Hydrol* X 4:100037

Wang L, Stuart ME, Bloomfield JP, Butcher AS, Gooddy DC, McKenzie AA et al (2012) Prediction of the arrival of peak nitrate concentrations at the water table at the regional scale in Great Britain. *Hydrol Process* 26(2):226–239. <https://doi.org/10.1002/hyp.8164>

Well R, Weymann D, Flessa H (2005) Recent research progress on the significance of aquatic systems for indirect agricultural N₂O emissions. *Environ Sci* 2(2–3):143–151. <https://doi.org/10.1080/15693430500393334>

Wilhelm E, Battino R, Wilcock RJ (1977) Low-pressure solubility of gases in liquid water. *Chem Rev* 77(2):219–262. <https://doi.org/10.1021/cr60306a003>

Zarnetske JP, Haggerty R, Wondzell SM, Baker MA (2011) Dynamics of nitrate production and removal as a function of residence time in the hyporheic zone. *J Geophys Res* 116(G1):G01025. <https://doi.org/10.1029/2010JG001356>

Zarnetske JP, Haggerty R, Wondzell SM (2015) Coupling multiscale observations to evaluate hyporheic nitrate removal at the reach scale. *Freshw Sci* 34(1):172–186. <https://doi.org/10.1086/680011>

Publisher's Note Springer Nature remains neutral with regard to jurisdictional claims in published maps and institutional affiliations.